

Robust Understanding of Human-Robot Social Interactions through Multimodal Distillation

Tongfei Bian
t.bian.1@research.gla.ac.uk
University of Glasgow
Glasgow, United Kingdom

Mathieu chollet
mathieu.chollet@glasgow.ac.uk
University of Glasgow
Glasgow, United Kingdom

Tanaya Guha*
tanaya.guha@glasgow.ac.uk
University of Glasgow
Glasgow, United Kingdom

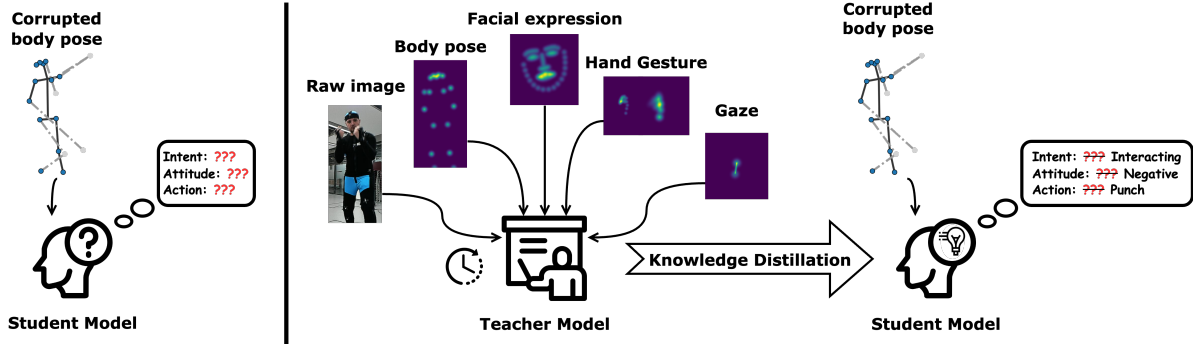


Figure 1: Our aim is to build a lightweight and robust model to understand human-robot social interactions. A novel teacher-student learning framework is built to achieve this, where the teacher model uses multimodal cues (body pose, face and hand gestures, and gaze) and raw RGB frames to learn a rich representation of the social scenario. Through knowledge distillation, the teacher model is able to transfer the knowledge to a lightweight student model that relies solely on body pose features. The student model is robust against incomplete and noisy inputs.

Abstract

The need for social robots and agents to interact and assist humans is growing steadily. To be able to successfully interact with humans, they need to understand and analyse socially interactive scenes from their (robot’s) perspective. Works that model social situations between humans and agents are few; and even those existing ones are often too computationally intensive to be suitable for deployment in real time or on real world scenarios with limited available information. We propose a robust knowledge distillation framework that models social interactions through various multimodal cues, yet is robust against incomplete and noisy information during inference. Our teacher model is trained with multimodal input (body, face and hand gestures, gaze, raw images) that transfers knowledge to a student model that relies solely on body pose. Extensive experiments on two publicly available human-robot interaction datasets demonstrate that our student model achieves an average accuracy gain of 14.75% over relevant baselines on multiple downstream social understanding tasks even with up to 51% of its input being corrupted. The student model is highly efficient: it is < 1% in size of the teacher model in terms of parameters and uses ~ 0.5% FLOPs of that in the teacher model. Our code will be made public during publication.

CCS Concepts

• **Human-centered computing** → **Human computer interaction (HCI)**; HCI theory, concepts and models.

Keywords

Human-Robot Interaction, Multimodal Learning, Knowledge Distillation, Egocentric Vision

1 Introduction

Recent application advances in social robotics and virtual agents include personal care, navigation, and user interaction [43]. A central challenge in social AI and human-robot interaction (HRI) is enabling the systems to understand and forecast human social behaviours from an egocentric perspective, such as intent to interact, attitudes, and social actions [6]. This capability is particularly critical during the early stages of interaction, where understanding the user’s engagement intent allows the system to proactively prepare for smooth and natural interactions. Early prediction enhances user experience and supports adaptive, context-aware responses [3]. However, deploying such predictive models in real-world settings remains challenging due to constraints in computational resources, input quality, and the need for real-time processing.

Understanding human social behaviours relies on multiple non-verbal signals [34], including body, face and hand gestures, gaze and raw images, each providing unique and complementary information into social interactions [41]. Despite progress in understanding multimodal nonverbal cues, several challenges remain in using them for broader social understanding in real-world deployment. **(1) Multimodal Integration:** Social understanding needs fusing information from diverse modalities that can sometimes be inconsistent. Models need to integrate information and differences across modalities to extract coherent semantic representations. **(2)**

Real-World Challenges: Egocentric perspectives introduce challenges such as limited field of view, camera motion, occlusions, and feature estimation errors, which degrades the reliability of social understanding. **(3) Computational Efficiency:** Using multiple modalities requires computationally intensive models and more feature estimation modules, posing difficulties for real-time inference on resource-constrained systems, such as social robots. Addressing these challenges needs a lightweight yet robust framework that can integrate multimodal cues under noisy conditions while supporting real-time social understanding.

To tackle these challenges, we propose a knowledge distillation framework that enables a lightweight student model to infer rich social cues from incomplete body pose input alone and jointly forecast three key aspects of social understanding: interaction intentions, attitudes, and social actions, as shown in Fig.1. Our approach consists of two stages: first, we train a teacher model with full-modal inputs, including body, face and hand gestures, gaze and raw images, to learn and output high-quality social representations. Then, we distil this knowledge into a lightweight student model that relies solely on body pose while incorporating spatio-temporal noise to simulate real-world data degradation. Instead of only learning from downstream task labels, the student also learns to infer multimodal and clean social cues through knowledge distillation, ensuring robust performance under noisy conditions. The lightweight design of the student model improves computational efficiency.

In summary, our work enhances the robustness and efficiency of jointly forecasting users' intent to interact, attitudes, and social actions from an egocentric perspective through the contributions:

- 1 **Knowledge distillation framework:** We propose a knowledge distillation framework where a teacher model SocialC3D using body, face and hand gestures, gaze and raw images, supervises a lightweight student model SocialEgoMobile that only uses body pose features. The average accuracy of the student model improved by 9.13% over independent training on JPL-Social [6] and 11.32% on the HARPER [4].
- 2 **Robustness to real-world noises:** To enhance robustness against noisy and incomplete input, we introduce spatiotemporal corruption for the student model. With knowledge distillation, when 51% of spatiotemporal information is lost the student maintains an average accuracy of 81.35% on JPL-Social [6] (14.68% improvement over independent training) and 59.05% on HARPER [4] (14.82% improvement).
- 3 **Efficiency and deployment readiness:** The proposed student model SocialEgoMobile demonstrates high computational efficiency, requiring only 1% of model parameters and 0.5% of the floating-point operations (FLOPs) compared to the teacher model.

2 Related Work

2.1 Social Intent Prediction

Egocentric social intent prediction is crucial for socially intelligent agents to establish natural, harmonious, and efficient interactions with users. A precise understanding of the user's social behaviour enables agents to timely adjust response strategies to meet user needs. Current research primarily models social intent as a binary classification task, focusing on predicting whether a user intends

to interact with an intelligent agent. Approaches include analyzing motor cues such as body orientation, movement direction, and speed [1], targeting users interested in interaction using visual and audible features [30], and using gaze information in virtual environments to infer interaction intent [8]. However, these methods are limited to distinguishing between 'interact' and 'not interact', failing to capture the richness and complexity of users' social intentions.

Human social intent estimation is inherently more nuanced than binary classifications and includes wider aspects. Recent research has explored various dimensions of users' social behaviours. Convolutional neural networks (CNNs) have been used to analyze facial expressions and body pose for attitude and emotion perception [18], while multilayer perceptions (MLPs) have been utilized to process facial and thermal images to infer user emotions during HRI [12]. Gated recurrent units (GRUs) capture the temporal dependencies of facial, acoustic, and textual features, enabling the detection of dynamic changes in users' attitudes and emotions during conversations [23]. Similarly, interaction action prediction has gained attention. Using cascade histogram of time series gradients can capture past spatio-temporal features and predict users' future social actions [32]. Social action and wider social signal in multi-agent scenarios have also been explored, by integrating body, facial, and hand pose features to capture user's body movement [6].

2.2 Non-Verbal Cues in Multimodal HRI

In Human-Robot Interaction (HRI), accurately interpreting the user's identity, social intent, behaviours, and communication requires integrating information from multiple modalities [41]. Meanwhile, non-verbal cues play a crucial role in understanding user intentions and needs [34]. For instance, while detecting sarcasm through text is challenging during a conversation, recognizing subtle body movements such as shoulder shrugs or lip curls allows humans to accurately identify sarcasm [7]. Consequently, capturing and interpreting multimodal non-verbal cues in HRI is essential for assessing the users. Recent research has explored various strategies for multi-modal fusion to enhance the accuracy of interaction models. For example, combining RGB images, facial expressions, and distance information can effectively assess user engagement [5] and interest [13] when interacting with service robots in public spaces. Facial expression and gaze information can be used to infer whether a user requires assistance in collaborative tasks [38]. To further improve robustness in real-world scenarios, researchers tried to model temporal information of non-verbal signals. Recurrent models have been used to model gestures and RGB video streams for identifying user action commands [25], and to detect user emotions during collaboration by analyzing body movements and facial expressions [28]. Pose skeletons and RGB information have been fused to predict interaction actions in single-user [19] and multi-user scenarios [40]. Non-verbal modalities including body, face, hand gestures, gaze and raw images provide rich contextual information that enhances a robot's ability to accurately understand to users' intentions, attitudes, and actions, improving the effectiveness of HRI systems.

Research gap. Despite the progress in social understanding using deep learning models, existing approaches often rely on multimodal inputs. However, processing more modal information increases

computational cost [24] and the deep models are sensitive to missing or noisy information [9], making them impractical for deployment on resource-constrained devices and real-world scenarios. While knowledge distillation has been explored to compress large models into lighter versions, most prior works focus on preserving accuracy under ideal conditions, overlooking the need to integrate multimodal information using a single modality and maintain robustness in environments with incomplete or degraded inputs [2]. To address these limitations, we propose a knowledge distillation framework with a lightweight, body pose-only student model that learns from a full-modality teacher model through a robust distillation, ensuring both computational efficiency and resilience to temporal and spatial noise.

3 Methodology

3.1 Problem Definition

Given a sequence of egocentric videos captured by an intelligent social agent, our aim is to forecast the user's social intent and behaviours in real time based only on the early stages of interaction (e.g., the first second). Specifically, we forecast the user's intent to interact, attitude, and social actions. To achieve this, we propose a knowledge distillation framework where a lightweight student model is trained to rely on body pose features, while a teacher model uses full multimodal inputs (body, face, hand gesture, gaze and raw images), as shown in Fig.2. Body pose features, facial keypoints, and hand keypoints are extracted from the video using Alphapose [11] and gaze features are extracted using MCGaze [15]. Formally, we define the input signals at step t as follows:

- $\mathbf{x}_t^{\text{Pose}}$: The coordinates of 17 body pose keypoints
- $\mathbf{x}_t^{\text{Image}}$: The raw images
- $\mathbf{x}_t^{\text{Face}}$: The coordinates of 68 facial keypoints
- $\mathbf{x}_t^{\text{Hand}}$: The coordinates of 42 hands keypoints
- $\mathbf{x}_t^{\text{Gaze}}$: The coordinates of the beginning and end of gaze

The **teacher model** F_{teacher} is trained with the complete set of input modalities:

$$R_{\text{teacher}} = F_{\text{teacher}}(\mathbf{x}_{t:T}^{\text{Pose}}, \mathbf{x}_{t:T}^{\text{Image}}, \mathbf{x}_{t:T}^{\text{Face}}, \mathbf{x}_{t:T}^{\text{Hand}}, \mathbf{x}_{t:T}^{\text{Gaze}}) \quad (1)$$

where R_t represents the high-level social representation extracted by the teacher model. To ensure efficiency and robustness, we introduce a lightweight student model F_{student} , which relies solely on body pose features $\mathbf{x}_t^{\text{Pose}}$:

$$R_{\text{student}} = F_{\text{student}}(\mathbf{x}_{t:T}^{\text{Pose}}) \quad (2)$$

where R_{student} represents the social representation extracted by the student model.

For the downstream tasks of forecasting user's intent to interact, attitude, and social actions, the social representations R extracted by the teacher or student model are processed by the **Chain** hierarchical classifier [6], which simulates how human understand and forecast social signals, predicting the results of three downstream tasks jointly:

$$\mathcal{L}_{\text{intent}}, \mathcal{L}_{\text{attitude}}, \mathcal{L}_{\text{action}} = \text{Classifier}(R) \quad (3)$$

3.2 Teacher Model

To effectively integrate multiple modalities, we employ a teacher model, SocialC3D which is based on PoseC3D [10], a spatio-temporal feature extraction framework using 3D convolutional neural networks (3D-CNN). PoseC3D converts sequences of 2D pose key-points into 3D heatmap stacks, according to their coordinates and confidence scores. The heatmaps are converted as follows:

$$H_i(x, y) = \exp\left(-\frac{(x - x_i)^2 + (y - y_i)^2}{2\sigma^2}\right) * c_i \quad (4)$$

where σ is the Gaussian variance of the heat map; (x, y) are the coordinates of the heatmap; (x_i, y_i) and c_i are the coordinates and confidence scores of the current keypoint i . This approach effectively captures spatio-temporal dependencies and exhibits greater robustness to noise than traditional skeleton-based methods. Additionally, the lateral connections between the RGB and Pose pathway fuse image and pose information, enhancing multimodal learning.

Based on this, we introduce SocialC3D to incorporate more modal information. SocialC3D transforms additional modalities, facial expressions, hand gestures, and gaze, into 3D heatmap stacks as input, which are processed using the same ResNet [16] as the body pose stream. For gaze estimation, we use the centre of the head bounding box as the beginning and calculate the end based on the gaze direction and the diagonal length of head bounding box. SocialC3D incorporate lateral connections to propagate intermediate representations across modalities at multiple stages, enabling deeper feature integration.

3.3 Student Model

The student model takes only body pose keypoints as input. Compared to raw visual information, body language provides a more direct and interpretable signal for understanding social interactions. Additionally, body posture inherently contain some facial and hand dynamics, allowing the model to integrate multimodal cues through knowledge distillation. Moreover, body pose features, as high-level abstractions, support lighter spatio-temporal analysis models and pose estimation, enhancing the student model's suitability for resource-constrained settings.

To reduce computational complexity while maintaining strong predictive performance, we developed **SocialEgoMobile** as our student model. To reduce the risk of overly deep networks amplifying noise and hindering useful information extraction, we designed a streamlined architecture consisting of a two-layer graphical attention network (GAT) [36] and a single-layer bi-directional long- and short-term memory (Bi-LSTM) [14]. By dynamically adjusting the attentional weights between neighbouring joints, GAT can effectively capture the spatial relationships between key points of the body pose skeleton graph, thus making the model more focused on useful information and limiting the noise. Meanwhile, Bi-LSTM enhances temporal modelling by processing sequences forward and backward with forgetting gates that can selectively filter noise. This lightweight yet effective design maintains stable performance under noisy and incomplete input conditions, thus enhancing robustness and making it suitable for real-time deployment in resource-limited environments.

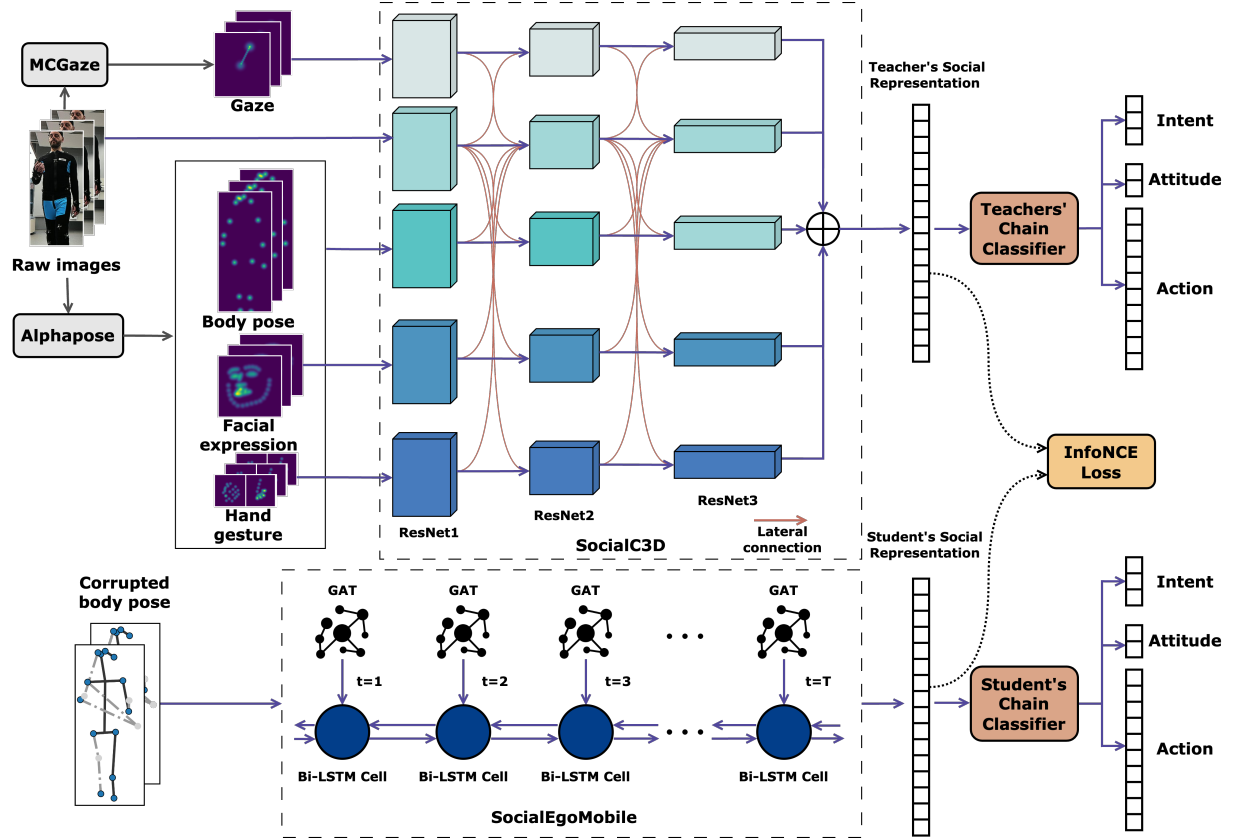


Figure 2: Our knowledge distillation framework uses SocialC3D as the teacher model, which fuses raw images, body, face, hand gestures, and gaze. Each modality is processed by a ResNet [16] and integrated via lateral connections and late fusion, producing a high-quality social representation for downstream tasks. The lightweight student model, SocialEgoMobile, uses only corrupted body pose. It consists of a two-layer GAT [36] and a single-layer Bi-LSTM [14] to extract social representations. The framework distillates knowledge from the teacher model by maximising the mutual information of the social representations output by the teacher and student model.

3.4 Knowledge Distillation

To effectively transfer knowledge of the user’s social behaviour from the teacher model to the student model, we adopt a feature-based knowledge distillation method. The student model learns not only from the ground truth labels of the downstream tasks but also by minimizing the discrepancy between its high-level social representations and those of the teacher model. We employ InfoNCE (Information Noise Contrastive Estimation) [27] to estimate and maximize the mutual information between teachers’ and students’ social representations. Specifically, InfoNCE enhances similarity between social representation of teacher and student models of the same input while reducing similarity between different inputs. During training, the loss function of the student model combines the mutual information loss from InfoNCE with the classification loss from the downstream tasks, weighted for back propagation. The loss of InfoNCE is defined as:

$$Loss_{infoNCE} = -\mathbb{E} \left[\log \frac{\exp(f(x, x^+))}{\sum_{x_j \in X} \exp(f(x, x_j))} \right] \quad (5)$$

where x is the teacher model’s social representation for a given input, x^+ is the representation from the student model for the same

input, and x_j is the representation from the student model for different inputs. The similarity function $f(x, x')$ is defined using cosine similarity as follows:

$$f(x, x') = \frac{x \cdot x'}{\|x\| \|x'\|} \quad (6)$$

By knowledge distillation, the student model can still learn high-level social knowledge from the teacher model with limited modality and corrupted inputs. Furthermore, we introduce spatio-temporal corruption in the student model’s input, enhancing its ability to integrate multimodal social cues while maintaining robustness to noise and missing data.

3.5 Input Corruption

In real-world applications, the social understanding model must not only work under the computational constraints of mobile platforms but also remain robust to incomplete and noisy inputs. To simulate such conditions, we deliberately introduce corruption in both spatial and temporal dimensions during training. In the spatial domain, a fixed number of body pose keypoints are randomly selected and corrupted by either setting their coordinate values and confidence scores to zero or replacing the coordinates with random

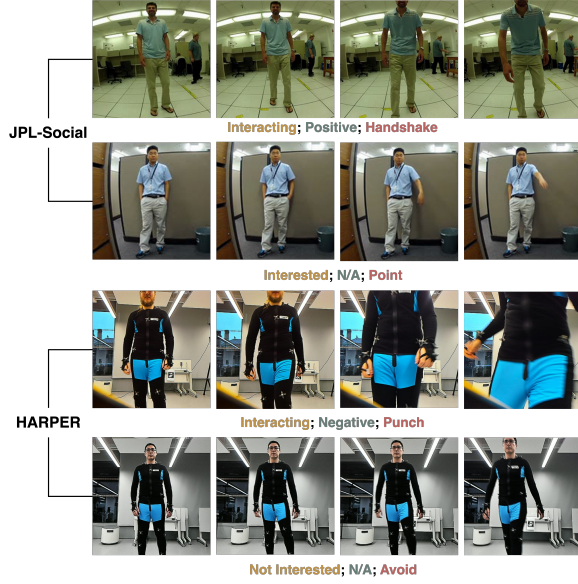


Figure 3: We standardized the input frame rate of two datasets to 10 FPS and limited the observation window to the first second of social interaction.

values within the normalized range. This mimics localized body occlusions or pose estimation errors. In the temporal domain, we randomly drop a fixed number of frames by setting all keypoint values in those frames to zero or normalized random noise, simulating transient global occlusions. These corruptions force the student model to learn robust representations and maintain performance under incomplete or noisy input during knowledge distillation.

4 Experiments

4.1 Data

To evaluate the performance and robustness of our models in forecasting users' social intents and behaviours from an egocentric perspective, we use two datasets of human-robot social interactions recorded from the robot's perspective. Examples of datasets are shown in Fig. 3.

JPL-Social [6] is an extension of the JPL-Interaction datasets [32, 33], designed for human-robot interaction research, with a focus on users' social actions within the central visual field. The original dataset captures 8 social actions performed by the main user: *handshake*, *hug*, *pet*, *wave*, *punch*, *throw*, *point*, and *leave*. JPL-Social extends this by annotating additional users in the field of view during multi-person scenarios, introducing two additional social actions: *gaze* and *no response*. Furthermore, JPL-Social provides labels for social intent (categorized as *interested*, *interacting*, or *not interested*) and attitude (*positive* or *negative*) for each user. The dataset comprises 290 interaction sequences involving 16 participants in diverse environmental settings.

HARPER [4] is a dataset capturing 10 human-robot social actions performed by 17 users, recorded from multiple perspectives using five cameras mounted on a quadrupedal robot. For our research, we use 6 social actions specifically relevant to robot-oriented interactions: *crash*, *walk-avoid*, *touch*, *walk-stop*, *punch*, and *kick*, so there are 260 interaction sequences. In addition, HARPER includes

variations in viewing angle and resolution, increasing the difficulty of understanding users' social signals. To ensure consistency in social representation, we manually annotated HARPER with the same social intent and attitude labels as JPL-Social.

4.2 Experiment Setting

We set the Frames Per Second (FPS) of the videos to 10 and limited the observation window to the first second of social interaction, which starts when the user approaches the social agent, so the inputs have 10 frames. To expand the training set, we randomly cropped video frames and re-extracted pose features, facial expressions, hand gestures, and gaze information. After horizontal flipping, we augmented number of videos 20 times for richer training data. We train and test the models on the two datasets separately. Given our focus on model efficiency, we report both the number of model parameters and the number of floating point operations (FLOPs) for each input.

4.3 Performance of the Teacher Model

As the teacher model, we compare SocialC3D with several state-of-the-art methods. Although originally designed for body pose skeleton graphs, these methods can also process facial and hand keypoint graphs. To ensure a fair comparison, we incorporated the raw image and gaze information channels from SocialC3D into all teacher models, aligning the available modalities across teacher models. Each modality channel in the teacher models is trained independently first and then during joint fine-tuning, outputs of all the channels are fused before being passed to the chain hierarchical classifier. To enhance body language understanding, the body pose and raw image channels of all teacher models are initialized with pre-trained weights on Kinetics 400 [20].

As shown in Table 1, we compare SocialC3D with SOTA methods on the JPL-Social and HARPER datasets. SocialC3D consistently achieves superior performance on three downstream social tasks in both datasets. Compared with the second-best model, MS-G3D [26], SocialC3D achieves an average accuracy improvement of 5.85% on JPL-Social and 5.77% on HARPER, which highlights the effectiveness of SocialC3D in understanding social cues and forecasting users' social intentions and behaviours from an egocentric perspective. We attribute this improvement to two key factors. First, instead of directly using pose features, converting them into heatmaps enhances robustness to pose estimation errors, which is particularly pronounced in egocentric settings due to narrow and jittery fields of view. Second, our experiments focus on the initial 10 frames of social interactions. 3D CNNs are suitable for capturing local temporal dynamics, making them more appropriate for our experiment setting. In contrast, models like ST-GCN [39] and MS-G3D [26] rely on complete and accurate pose features, making them more vulnerable to missing joints and estimation noise. ST-TR [29], while effective in modelling long-term dependencies due to using transformers [35], struggles with short sequences and lacks mechanisms to handle input degradation. Although SocialEgoNet [6] is designed to capture users' non-verbal social cues from an egocentric perspective, its lightweight architecture limits its capacity to extract fine-grained information independently.

| Model | Params (M) | FLOPs (M) | JPL-Social | | | HARPER | | |
|-------------------------------|---------------|--------------|--------------|---------------|--------------|--------------|---------------|--------------|
| | | | Intent Acc. | Attitude Acc. | Action Acc. | Intent Acc. | Attitude Acc. | Action Acc. |
| ST-GCN ⁺ [39] | 43.86 | 1924.87 | 86.90 | 76.19 | 71.43 | 86.54 | 73.08 | 78.85 |
| ST-TR ⁺ [29] | 58.48 | 4724.63 | 79.76 | 59.52 | 48.81 | 75.00 | 65.38 | 59.61 |
| MS-G3D ⁺ [26] | 48.82 | 5241.97 | 88.10 | 80.95 | 76.19 | 90.38 | 78.85 | 80.77 |
| SocialEgoNet ⁺ [6] | 37.78 | 422.35 | 86.90 | 77.38 | 71.43 | 86.54 | 75.00 | 78.85 |
| SocialC3D (ours) | 48.49 | 7902.19 | 92.85 | 88.10 | 82.14 | 96.15 | 82.69 | 88.46 |
| SocialEgoMobile (ours) | 0.43 | 4.23 | 82.14 | 71.43 | 67.86 | 69.23 | 44.23 | 51.92 |

Table 1: Comparison of SocialC3D and SocialEgoMobile with state-of-the-art methods on the JPL-Social and HARPER. SocialEgoMobile relies solely on clean body pose features as input. '+' indicates that the model uses raw image and gaze information.

In addition, we report the performance of SocialEgoMobile using only body pose to compare its accuracy and computational efficiency against the teacher models. Compared to SocialC3D, SocialEgoMobile's average accuracy of downstream tasks on JPL-Social was 13.89% lower and 33.97% lower on HARPER. The larger performance gap on HARPER is attributed to its recording setup, where the robot dog has a lower vantage point and fewer frames with full-body visibility, resulting in noisier and more incomplete pose inputs, as shown in Fig.3. In terms of computational efficiency, compared to SocialC3D, SocialEgoMobile only needs 0.98% of the model parameters and 0.54% of FLOPs. These results show SocialEgoMobile is computationally lightweight enough for social understanding on mobile platforms with limited resources.

4.4 Robustness Analysis on the Student Model

To address the practical challenges faced by mobile socially intelligent agents from an egocentric perspective, such as occlusion of user body parts and pose estimation error, we deliberately introduced random spatio-temporal corruption into the input of the student model SocialEgoMobile, as mentioned in Section 3.5. The goal is to improve robustness by using the rich and clean knowledge extracted from the intermediate social representations of the teacher model SocialC3D, to supervise the learning of the student model with corrupted inputs. During the robustness tests, student models were trained for 70 epochs. The first 30 epochs are warm-up phase, where the corruption rate was gradually increased to the final value to prevent unstable training due to excessive information loss.

Fig.4 compares SocialEgoMobile's performance under two settings: independent learning and knowledge distillation. Under independent learning, performance degrades as corruption increases. When 30% of joints and frames is corrupted, $30\% \oplus 30\% = 51\%$ of the information in the input was corrupted. The average accuracy across three downstream tasks drops by 8.85%, demonstrating the increased difficulty and robustness demands. In contrast, with knowledge distillation, SocialEgoMobile consistently outperforms the independently trained counterpart across all input settings. When 30% of joints and frames is corrupted, SocialEgoMobile trained via distillation surpasses the performance of the independently trained model using clean input. This suggests that knowledge distillation effectively transfers social knowledge from the teacher model, which incorporates additional modalities and complete, clean inputs, to the student model. So it can more accurately capture valuable social cues even when facing corrupted inputs.

The performance gains are particularly significant for the user attitude and social action prediction tasks, which rely more on detailed and accurate input.

Whether trained independently or via knowledge distillation, SocialEgoMobile is more sensitive to the corruption of spatial information than temporal information. This is because temporal patterns in human behaviour tend to be more regular and predictable, allowing models to more effectively compensate for missing frames and filter out noise. In contrast, spatial patterns of pose graphs are more complex, such as body structure and human kinematics.

4.5 Ablation Experiments

Contribution of Multi-Modalities. We incorporate body pose, raw images, face, hand gestures, and gaze as input modalities for the teacher model SocialC3D, enabling it to comprehensively capture social cues from users' non-verbal behaviours across multiple perspectives. Body pose and raw images are the foundational modalities and prior work has demonstrated their effectiveness and complementarity in understanding body movements [10]. In contrast, facial expressions, hand gestures, and gaze focus on localized regions of the body, providing fine-grained cues essential for capturing nuanced social signals.

Fig.5 illustrates SocialC3D's performance across three downstream tasks with full modality and with each of the three localized modalities ablated. The **Attitude** and **Intent** tasks show performance degradation when facial information is removed. Facial orientation offers cues about a user's attention, while expressions convey emotional states that differentiate social behaviours with similar body movements in early stages, such as 'throw' and 'wave hands'. The **Action** task is more sensitive to the absence of hand gestures, as detailed hand pose information helps the model to distinguish between fine-grained actions, such as the differences in finger closure for 'touch' and 'handshake'. For the **Intent** task, the lack of gaze information leads to the greatest drop in accuracy, since gaze direction directly reflects user focus and intention. While facial orientation may offer partial substitutes, it cannot fully replicate the precision of direct gaze signals. Through knowledge distillation, the impact of missing modalities observed in the teacher model is transferred to the student model, as shown in Fig.5. These results confirm that the proposed knowledge distillation framework successfully transfers the integrated multimodal social knowledge from the teacher model to the unimodal student model.

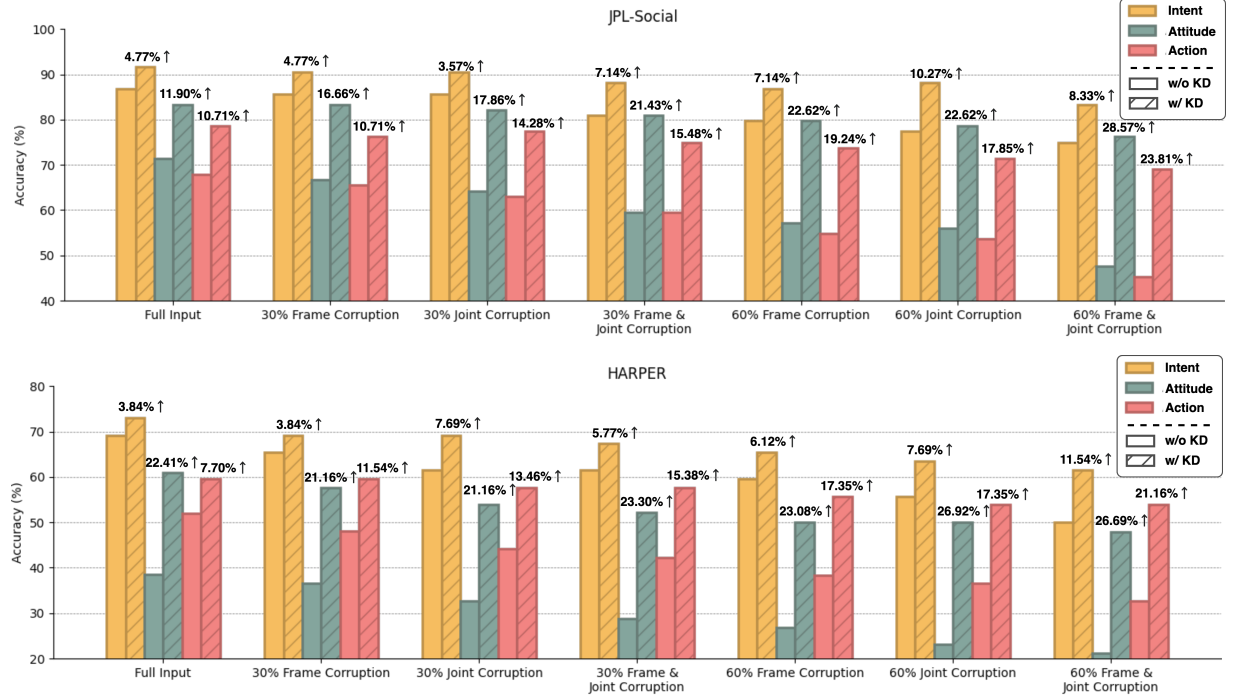


Figure 4: Knowledge distillation (KD) consistently improves the performance of the student model, SocialEgoMobile, under Individual and simultaneous spatio-temporal corruption on all three downstream tasks, interaction intent, attitude, and social action forecast. Improvements on downstream task accuracy through distillation are labelled.

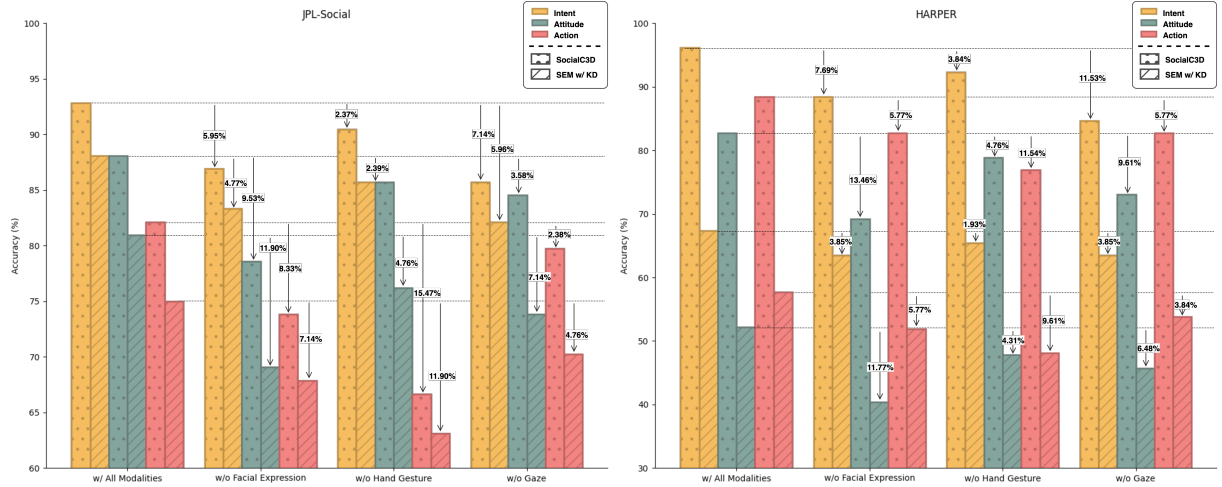


Figure 5: Performance comparison on JPL-Social and HARPER of SocialC3D using different input modalities, and the impact of corresponding SocialC3D-based Knowledge Distillation on SocialEgoMobile (SEM) when 30% of spatio-temporal information are corrupted. Accuracy drops due to missing modalities are labelled.

Distillation Methods. In Table 2, we compare the performance improvements brought by different knowledge distillation methods to the student model, SocialEgoMobile, when 30% of joints and frames are corrupted. Distillation based on intermediate features outperforms soft label distillation, as the student model in our experiments must learn to integrate information of additional modalities from high-level social representation provided by the teacher model and compensate for the impact of missing or noisy

inputs. Learning only from the teacher’s output distributions is insufficient. Among the intermediate feature-based methods, InfoNCE [27] achieves the best performance. By maximizing mutual information between the teacher and student model’s intermediate social representations, InfoNCE encourages the student to learn semantically aligned features, rather than enforcing exact numerical matching at lower levels. This is suitable for our experiment setting, where the teacher and student operate on different input

| Distillation Method | JPL-Social | | | HARPER | | |
|-------------------------|--------------|---------------|--------------|--------------|---------------|--------------|
| | Intent Acc. | Attitude Acc. | Action Acc. | Intent Acc. | Attitude Acc. | Action Acc. |
| w/o KD | 80.95 | 59.52 | 59.52 | 61.54 | 28.84 | 42.31 |
| Soft Label [17] | 82.14 | 71.43 | 64.29 | 61.54 | 39.13 | 44.23 |
| Attention Transfer [42] | 84.52 | 73.81 | 69.05 | 63.46 | 39.13 | 48.08 |
| FitNet [31] | 84.52 | 76.19 | 66.67 | 65.38 | 43.48 | 48.08 |
| KDGAN [37] | 88.10 | 78.57 | 69.05 | 65.38 | 43.48 | 50.00 |
| InfoNCE [27] | 88.10 | 80.95 | 75.00 | 67.31 | 52.14 | 57.69 |

Table 2: Comparison of different knowledge distillation methods when 30 % of joints and frames are corrupted.

| Model Architecture | JPL-Social | | |
|-----------------------------|--------------|--------------|--------------|
| | Intent F1 | Attitude F1 | Action F1 |
| SocialEgoMobile | 88.10 | <u>80.95</u> | 75.00 |
| w/ 3 layers GAT | 84.52 | 76.19 | 69.05 |
| w/ 1 layers GAT | 83.33 | 69.05 | 67.86 |
| w/ 2 layer GCN [21] | 85.71 | 71.43 | 67.86 |
| w/ 2 layers Bi-LSTM | 88.10 | 82.14 | 75.00 |
| w/ 1 layer TCN [22] | 83.33 | 69.05 | 65.48 |
| w/ 1 layer Transformer [35] | 77.38 | 66.67 | 54.76 |

Table 3: Performance Comparison of SocialEgoMobile with Different Backbone Models on JPL-Social when 30% joints and frames are corrupted. The best results are shown in bold and the second best results are underlined.

modalities and the student receives incomplete and noisy inputs, making low-level alignment impractical. InfoNCE promotes the alignment of high-level semantic information, leading to better noise tolerance and generalization.

Student Model Architecture. To enhance the robustness and efficiency of processing noisy pose feature sequences, we designed the student model SocialEgoMobile with a two-layer GAT [36] followed by a one-layer Bi-LSTM [14]. Table 3 presents a comparison of different model configurations under the knowledge distillation with corrupted inputs. In the spatial dimension, a two-layer GAT achieves a good trade-off between expressiveness and stability. Fewer layers limit the receptive field, reducing the model’s ability to capture global graph structural patterns, while deeper GATs tend to propagate noise more widely. Moreover, GAT’s adaptive attention mechanism enables selective aggregation of useful information from neighbouring nodes, offering greater resilience to noisy or missing joints compared to standard GCNs [21]. In the temporal dimension, a single-layer Bi-LSTM provides sufficient modelling capacity for short pose feature sequences, while deeper Bi-LSTMs introduce additional parameters with marginal performance improvement. Compared to TCNs [22] and Transformers [35], Bi-LSTM is better suited for sequential data with inherent temporal dependencies and benefits from its gating mechanism, which improves robustness to sparsity and temporal discontinuity. Overall, the combination of two GAT layers and one Bi-LSTM in SocialEgoMobile offers an effective balance between expressiveness, robustness, and computational efficiency.

4.6 Key Takeaways

To summarize our results, we highlight three main observations:

- The proposed teacher model SocialC3D effectively integrates multimodal inputs (body, face, hand, gaze and raw image) for egocentric social understanding, surpassing SOTAs. Each modality contributes unique and complementary information.
- The knowledge distillation framework enables the student model to absorb multimodal and clean knowledge from the teacher, improving its ability of capture meaningful information and robustness against spatial-temporal noisy data.
- The distilled student SocialEgoMobile achieves a trade-off between performance, robustness, and computational cost, which is suitable for deployment on resource-constrained systems.

5 Conclusion

In this paper, we address the challenges of performance, robustness, and computational efficiency in forecasting users’ social interaction intentions and behaviours from an egocentric perspective on mobile platforms or embedding system. We propose SocialEgoMobile, a lightweight social cue understanding model based on knowledge distillation. In our knowledge distillation framework, the teacher model, SocialC3D, uses multimodal inputs, including body poses, raw images, facial expressions, hand gestures, and gaze patterns, while the student model only relies on deliberate corrupted body pose features. By distilling knowledge from the teacher model’s integrated multimodal representations and downstream task supervision, the student model learns to produce robust predictions under noisy and incomplete input conditions. This work offers an effective and lightweight solution for real-time social understanding, particularly suited for resource-constrained scenarios such as social robots and intelligence social agents. Future work will focus on further enhancing the model’s robustness through real-world deployment and investigating its generalization to complex scenarios, including domain adaptation across viewpoints and environments.

References

- [1] Gabriele Abbate, Alessandro Giusti, Viktor Schmuck, Oya Celiktutan, and Antonio Paolillo. 2024. Self-supervised prediction of the intention to interact with a service robot. *Robotics and Autonomous Systems* 171 (2024), 104568.
- [2] Elahe Arani, Fahad Sarfraz, and Bahram Zonooz. 2021. Noise as a resource for learning in knowledge distillation. In *Proceedings of the IEEE/CVF Winter Conference on Applications of Computer Vision*. 3129–3138.
- [3] João Avelino, Leonel Garcia-Marques, Rodrigo Ventura, and Alexandre Bernardino. 2021. Break the ice: a survey on socially aware engagement for human-robot first encounters. *International Journal of Social Robotics* 13, 8 (2021), 1851–1877.
- [4] Andrea Avogaro, Andrea Toaiari, Federico Cunico, Xiangmin Xu, Haralambos Dafas, Alessandro Vinciarelli, Emma Li, and Marco Cristani. 2024. Exploring 3D Human Pose Estimation and Forecasting from the Robot's Perspective: The HARPER Dataset. In *2024 IEEE/RSJ International Conference on Intelligent Robots and Systems (IROS)*. IEEE, 5828–5835.
- [5] Atef Ben-Youssef, Giovanna Varni, Slim Essid, and Chloé Clavel. 2019. On-the-fly detection of user engagement decrease in spontaneous human-robot interaction using recurrent and deep neural networks. *International Journal of Social Robotics* 11, 5 (2019), 815–828.
- [6] Tongfei Bian, Yiming Ma, Mathieu Chollet, Victor Sanchez, and Tanaya Guha. 2025. Interact with me: Joint Egocentric Forecasting of Intent to Interact, Attitude and Social Actions. In *Proceedings of the IEEE International Conference on Multimedia and Expo (ICME)*.
- [7] Santiago Castro, Devamanyu Hazarika, Verónica Pérez-Rosas, Roger Zimmermann, Rada Mihalcea, and Soujanya Poria. 2019. Towards Multimodal Sarcasm Detection (An „Obviously“ Perfect Paper). In *Proceedings of the 57th Annual Meeting of the Association for Computational Linguistics*. 4619–4629.
- [8] Brendan David-John, Candace Peacock, Ting Zhang, T Scott Murdison, Hrvoje Benko, and Tanya R Jonker. 2021. Towards gaze-based prediction of the intent to interact in virtual reality. In *ACM symposium on eye tracking research and applications*. 1–7.
- [9] Nathan Drenkow, Numair Sani, Ilya Shpitser, and Mathias Unberath. 2021. A systematic review of robustness in deep learning for computer vision: Mind the gap? *arXiv preprint arXiv:2112.00639* (2021).
- [10] Haodong Duan, Yue Zhao, Kai Chen, Dahua Lin, and Bo Dai. 2022. Revisiting skeleton-based action recognition. In *Proceedings of the IEEE/CVF conference on computer vision and pattern recognition*. 2969–2978.
- [11] Hao-Shu Fang, Jiefeng Li, Hongyang Tang, Chao Xu, Haoyi Zhu, Yuliang Xiu, Yong-Lu Li, and Cewu Lu. 2022. Alphapose: Whole-body regional multi-person pose estimation and tracking in real-time. *IEEE transactions on pattern analysis and machine intelligence* 45, 6 (2022), 7157–7173.
- [12] Chiara Filippini, Edoardo Spadolini, Daniela Cardone, Domenico Bianchi, Maurizio Preziuso, Christian Sciarretta, Valentina Del Cimmuto, Davide Lisciani, and Arcangelo Merla. 2021. Facilitating the child-robot interaction by endowing the robot with the capability of understanding the child engagement: The case of mio amico robot. *International Journal of Social Robotics* 13 (2021), 677–689.
- [13] Mary Ellen Foster, Bart Craenen, Amol Deshmukh, Oliver Lemon, Emanuele Bastianelli, Christian Dondrup, Ioannis Papaioannou, Andrea Vanzo, Jean-Marc Odobez, Olivier Canévet, et al. 2019. MuMMER: Socially Intelligent Human-Robot Interaction in Public Spaces. In *Artificial Intelligence for Human-Robot Interaction Symposium (AI-HRI)*.
- [14] Alex Graves and Jürgen Schmidhuber. 2005. Frameworkwise phoneme classification with bidirectional LSTM networks. In *Proceedings. 2005 IEEE International Joint Conference on Neural Networks, 2005*, Vol. 4. IEEE, 2047–2052.
- [15] Yiran Guan, Zhuoguang Chen, Wenzheng Zeng, Zhiguo Cao, and Yang Xiao. 2023. End-to-End Video Gaze Estimation via Capturing Head-Face-Eye Spatial-Temporal Interaction Context. *IEEE Signal Processing Letters* 30 (2023), 1687–1691.
- [16] Kaiming He, Xiangyu Zhang, Shaoqing Ren, and Jian Sun. 2016. Deep residual learning for image recognition. In *Proceedings of the IEEE conference on computer vision and pattern recognition*. 770–778.
- [17] Geoffrey Hinton, Oriol Vinyals, and Jeff Dean. 2015. Distilling the Knowledge in a Neural Network. *stat* 1050 (2015), 9.
- [18] Chaudhary Muhammad Aqdas Ilyas, Rita Nunes, and Thomas B Moeslund. 2021. Deep Emotion Recognition through Upper Body Movements and Facial Expression.. In *VISIGRAPP (5: VISAPP)*. 669–679.
- [19] Md Mofijul Islam and Tariq Iqbal. 2020. Hamlet: A hierarchical multimodal attention-based human activity recognition algorithm. In *2020 IEEE/RSJ International Conference on Intelligent Robots and Systems (IROS)*. IEEE, 10285–10292.
- [20] Will Kay, Joao Carreira, Karen Simonyan, Brian Zhang, Chloe Hillier, Sudheendra Vijayanarasimhan, Fabio Viola, Tim Green, Trevor Back, Paul Natsev, et al. 2017. The kinetics human action video dataset. *arXiv preprint arXiv:1705.06950* (2017).
- [21] Thomas N. Kipf and Max Welling. 2017. Semi-Supervised Classification with Graph Convolutional Networks. In *Proc ICLR*.
- [22] Colin Lea, Michael D Flynn, Rene Vidal, Austin Reiter, and Gregory D Hager. 2017. Temporal convolutional networks for action segmentation and detection. In *proceedings of the IEEE Conference on Computer Vision and Pattern Recognition*. 156–165.
- [23] Yuanhao Li, Tianyu Zhao, and Xun Shen. 2020. Attention-Based Multimodal Fusion for Estimating Human Emotion in Real-World HRI. In *Companion of the 2020 ACM/IEEE International Conference on Human-Robot Interaction (HRI '20)*. Association for Computing Machinery, 340–342.
- [24] Paul Pu Liang, Amir Zadeh, and Louis-Philippe Morency. 2024. Foundations & trends in multimodal machine learning: Principles, challenges, and open questions. *Comput. Surveys* 56, 10 (2024), 1–42.
- [25] Hongyi Liu, Tongtong Fang, Tianyu Zhou, and Lihui Wang. 2018. Towards robust human-robot collaborative manufacturing: Multimodal fusion. *IEEE Access* 6 (2018), 74762–74771.
- [26] Ziyu Liu, Hongwen Zhang, Zhenghao Chen, Zhiyong Wang, and Wanli Ouyang. 2020. Disentangling and unifying graph convolutions for skeleton-based action recognition. In *Proceedings of the IEEE/CVF conference on computer vision and pattern recognition*. 143–152.
- [27] Aaron van den Oord, Yazhe Li, and Oriol Vinyals. 2018. Representation learning with contrastive predictive coding. *arXiv preprint arXiv:1807.03748* (2018).
- [28] John Páez and Enrique González. 2022. Human-robot scaffolding: An architecture to foster problem-solving skills. *ACM Transactions on Human-Robot Interaction (THRI)* 11, 3 (2022), 1–17.
- [29] Chiara Plizzari, Marco Cannici, and Matteo Matteucci. 2021. Spatial temporal transformer network for skeleton-based action recognition. In *Pattern recognition. ICPR international workshops and challenges: virtual event, January 10–15, 2021, Proceedings, Part III*. Springer, 694–701.
- [30] Shokoofeh Pourmehr, Jack Thomas, Jake Bruce, Jens Wawerla, and Richard Vaughan. 2017. Robust sensor fusion for finding HRI partners in a crowd. In *2017 IEEE International Conference on Robotics and Automation (ICRA)*. 3272–3278.
- [31] Adriana Romero, Nicolas Ballas, Samira Ebrahimi Kahou, Antoine Chassang, Carlo Gatta, and Yoshua Bengio. 2014. Fitnets: Hints for thin deep nets. *arXiv preprint arXiv:1412.6550* (2014).
- [32] Michael S Ryoo, Thomas J Fuchs, Lu Xia, Jake K Aggarwal, and Larry Matthies. 2015. Robot-centric activity prediction from first-person videos: What will they do to me?. In *Proceedings of the tenth annual ACM/IEEE international conference on human-robot interaction*. 295–302.
- [33] Michael S Ryoo and Larry Matthies. 2013. First-person activity recognition: What are they doing to me?. In *Proceedings of the IEEE conference on computer vision and pattern recognition*. 2730–2737.
- [34] Jacqueline Urakami and Katie Seaborn. 2023. Nonverbal cues in human-robot interaction: A communication studies perspective. *ACM Transactions on Human-Robot Interaction* 12, 2 (2023), 1–21.
- [35] Ashish Vaswani, Noam Shazeer, Niki Parmar, Jakob Uszkoreit, Llion Jones, Aidan N Gomez, Łukasz Kaiser, and Illia Polosukhin. 2017. Attention is all you need. *Advances in neural information processing systems* 30 (2017).
- [36] Petar Veličković, Guillem Cucurull, Arantxa Casanova, Adriana Romero, Pietro Liò, and Yoshua Bengio. 2018. Graph Attention Networks. In *International Conference on Learning Representations*.
- [37] Xiaojie Wang, Rui Zhang, Yu Sun, and Jianzhong Qi. 2018. Kdgan: Knowledge distillation with generative adversarial networks. *Advances in neural information processing systems* 31 (2018).
- [38] Jason R Wilson, Phyto Thuta Aung, and Isabelle Boucher. 2022. When to help? A multimodal architecture for recognizing when a user needs help from a social robot. In *International Conference on Social Robotics*. Springer, 253–266.
- [39] Sijie Yan, Yuanjun Xiong, and Dahua Lin. 2018. Spatial temporal graph convolutional networks for skeleton-based action recognition. In *Proceedings of the AAAI conference on artificial intelligence*, Vol. 32.
- [40] Mohammad Samin Yasar, Md Mofijul Islam, and Tariq Iqbal. 2024. IMPRINT: Interactional dynamics-aware motion prediction in teams using multimodal context. *ACM Transactions on Human-Robot Interaction* 13, 3 (2024), 1–29.
- [41] Zerrin Yumak and Nadia Magnenat-Thalmann. 2015. Multimodal and multi-party social interactions. In *Context aware human-robot and human-agent interaction*. Springer, 275–298.
- [42] Sergey Zagoruyko and Nikos Komodakis. 2017. Paying More Attention to Attention: Improving the Performance of Convolutional Neural Networks via Attention Transfer. In *International Conference on Learning Representations*.
- [43] Chen Zhou, Ming-Cheng Miao, Xin-Ran Chen, Yi-Fei Hu, Qi Chang, Ming-Yuan Yan, and Shu-Guang Kuai. 2022. Human-behaviour-based social locomotion model improves the humanization of social robots. *Nature Machine Intelligence* 4, 11 (2022), 1040–1052.